22.0 Quantum Optics and Photonics

Academic and Research Staff

Prof. S. Ezekiel, Dr. P.R. Hemmer, Dr. M.G. Prentice, Dr. H. Lamela-Rivera, B. Bernacki, D. Morris, J. Kierstead

Graduate Students

R. Barat, M.S. Shahriar, S.P. Smith, F. Zarinetchi

Undergraduate Students

J. Bevilaqua, T. Hawkeye, J. Kuchar, M.C. Neils

Sponsors

Joint Services Electronics Program (Contract DAAL03-86-K-0002)
National Science Foundation (Grant PHY 82-10369)
U.S. Air Force - Office of Scientific Research (Contract F49620-82-C-0091)
U.S. Air Force - Rome Air Development Center

22.1 Measurement of Fresnel-Drag in Moving Media Using Aring Resonator Technique

It has been known for many years that the observed velocity of light in a moving medium differs from that in a stationary medium. This effect, namely the Fresnel-drag, was explained by the special theory of relativity. While special relativity has been very accurately tested, no tests of comparable precision can be claimed regarding the theory's predictions for light propagation in moving media.

We have performed careful measurements of the Fresnel-drag in various moving glass media and tested the dependence of the drag coefficient on refractive index and dispersion. A solid medium was used in our experiments to provide a precisely known velocity and index. To further ensure the accuracy of these measurements we have studied the drag dependence on other key parameters such as the thickness and velocity of the glass samples, as well as the angle between the light beam and glass normal.

Our technique is based on moving a glass plate of known index and dispersion back and forth inside a ring resonator as shown in figure 22.1. In this way, the Fresnel-drag generated by the motion of the glass induces a nonreciprocal phase shift which manifests itself as a difference in the resonance frequencies of the cavity for oppositely propagating field directions. The precision measurement of small resonance frequency difference in a ring cavity is similar to the measurement of nonreciprocal phase shift due to inertial rotation, i.e., Sagnac effect.

The effective drag coefficient was measured for four glass samples namely; BK-7, SF-1, SF-57 and fused silica which have different indices of refraction and dispersion. Averaging fifteen separate measurements resulted in an overall agreement with theory

that was well within our $\pm$ 2.8x10^{-4} measurement uncertainty, thus verifying the drag dependence on both the refractive index as well as the dispersion of the moving medium. These measurements provided the most accurate verification of Fresnel-drag thus far.

The use of a solid medium together with ac detection techniques contributed to the improved experimental verification of the Fresnel-drag reported here. Aside from varying sample index and dispersion we also varied sample thickness, velocity and angle of incidence. Further improvement in the accuracy of the measurements can be made by placing the cavity within an evacuated chamber to exclude air currents, and by using a smoother bearing for guiding the motion of the glass sample.

Publication

Sanders, G.A., and S. Ezekiel, "Measurement of Fresnel-Drag in Moving Media Using a Ring Resonator Technique," *J. Opt. Soc Am. B* (1988), to be published).

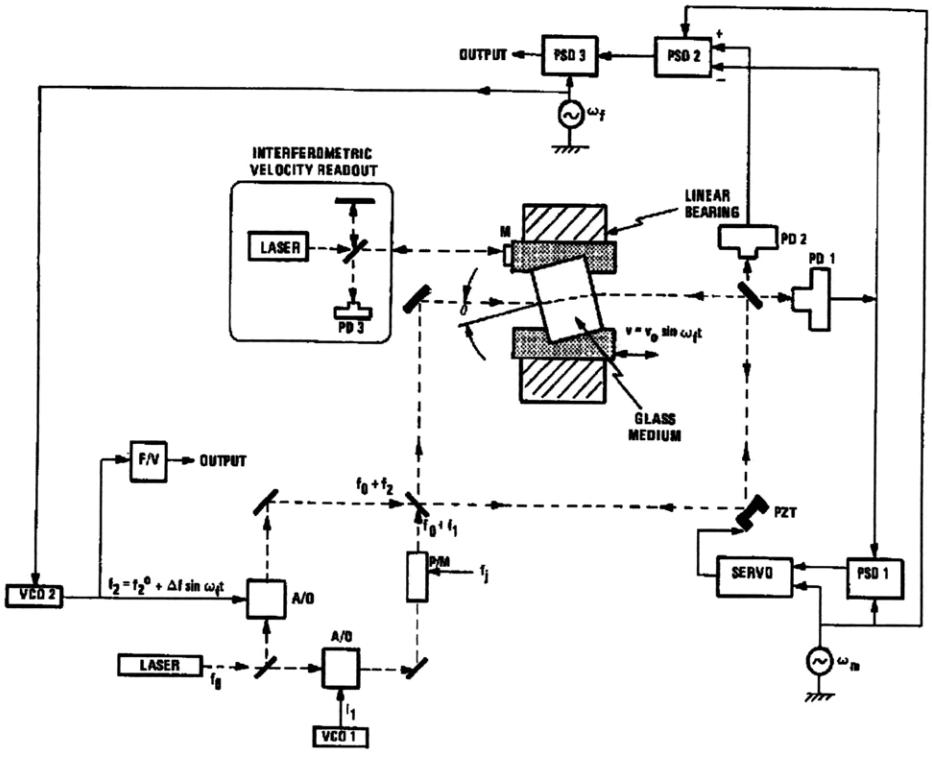

Figure 22.1 Experimental setup.

22.2 Observation of Ultra-Narrow Raman Ramsey Fringes in a Cesium Atomic Beam Using a Semiconductor Laser

We have observed an ultra narrow, 4 kHz wide Raman Ramsey fringe in a cesium atomic beam using a semiconductor laser with a free running linewidth of 45 MHz. To

our knowledge, this is the narrowest atomic resonance recorded using a semiconductor laser and has applications in the development of new time and frequency standards. A clock based on the resonance Raman effect in cesium could be smaller, simpler and less expensive than a conventional cesium clock.

The stimulated resonance Raman process is illustrated in figure 22.2 where we show a Raman transition between two long-lived states, 1 and 3, induced by two laser fields at frequencies ω_1 and ω_2. As is well-known, the Raman transition linewidth for weak copropagating laser fields is primarily determined by the decay rates of the long lived states 1 and 3. Thus, the linewidth is set by the transit time. To achieve an effectively long transit time, and thus a very narrow linewidth, Ramsey's technique of separated field excitation is used.

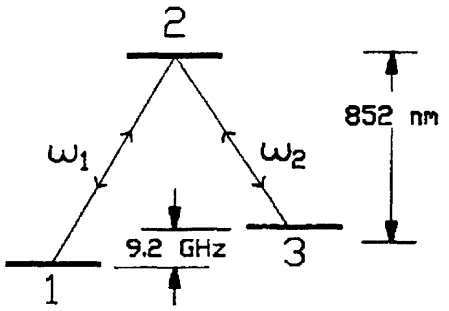

Figure 22.2 Schematic of Raman transition in cesium.

In our present experiment, the long-lived states 1 and 3 in figure 22.2 are respectively the $6^2S_{1/2}(F = 3)$ and $(F=4)$ ground state hyperfine levels in cesium separated by 9.2 GHz, and state 2 is the $6^2P_{3/2}(F = 4)$ level. The optical transitions are components of the cesium D_2 line at 852 nm.

The experimental setup is shown schematically in figure 22.3. The laser diode is a single frequency, double heterostructure, AlGaAs laser (Hitachi HLP-1400) operating at 852 nm and mounted on a thermoelectric device. The linewidth of the laser was 45 MHz as measured by a Fabry Perot interferometer.

Generation of the two optical fields, ω_1 and ω_2 is accomplished by modulating the laser current at 4.6 GHz with a microwave VCO, shown in figure 22.3, thus yielding two amplitude modulation sidebands separated by 9.2 GHz. By generating ω_1 and ω_2 in this manner, the effect of laser jitter can be eliminated. In our previous work using a sodium beam and a dye laser, the second optical field was generated by frequency shifting in an external Bragg cell.

Figure 22.4(a) shows the modulation sidebands of the modulated laser as measured by a short, plane-parallel, scanning Fabry-Perot cavity with a free spectral range of 25 GHz. As can be seen, the separation between sidebands is 4.6 GHz and that there is no evidence of any laser instabilities. In contrast, figure 22.4(b) shows the spectrum of the unmodulated single mode laser.

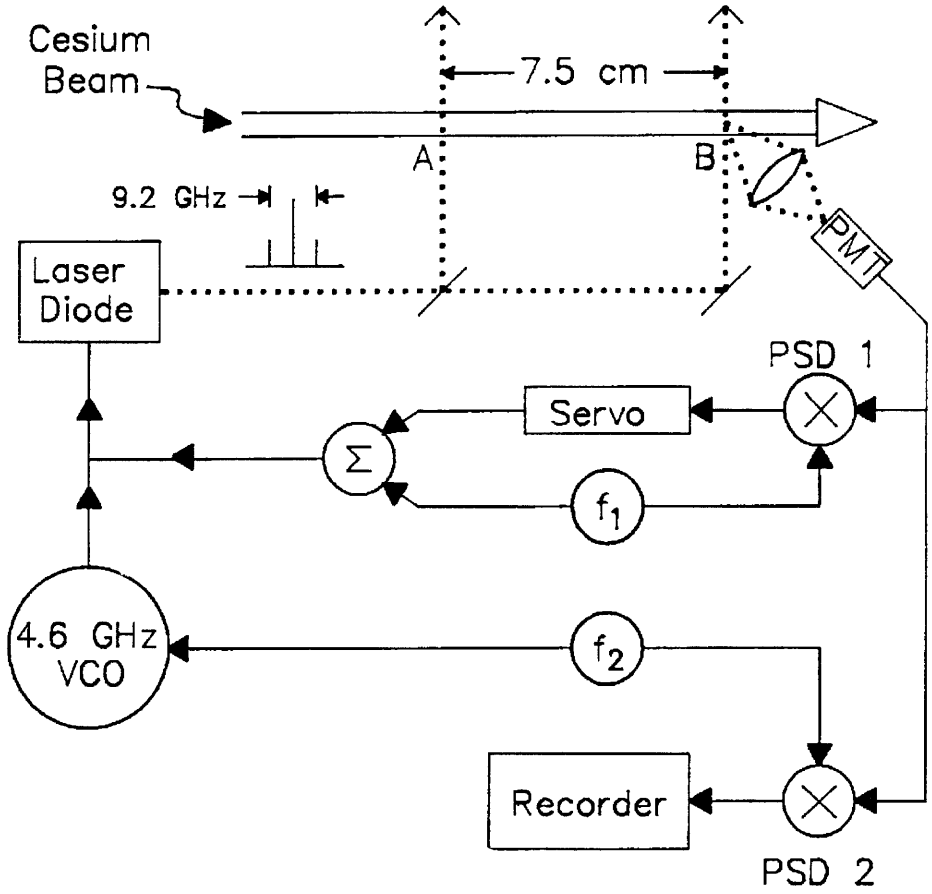

Figure 22.3. Experimental setup.

As indicated in figure 22.3, the output from the modulated laser interacts with the cesium atomic beam in zones "A" and "B," and the fluorescence from zone "B" is collected onto a photomultiplier tube. Figure 22.5 shows the demodulated fluorescence from zone "B" which exhibits the Ramsey fringes as the microwave oscillator is slowly swept through the center of one of the cesium Zeeman transitions. As shown in the figure, the central fringe has a width of 4 kHz, which is in good agreement with the predicted width for a 7.5 cm zone separation and a 200°C oven temperature. To observe the Raman transition, the laser and sidebands were held by means of a servo near the maximum of the fluorescence lineshape in zone "B." It should be noted that these Ramsey fringes are still preliminary and the details of the fringe shapes have yet to be carefully investigated.

As in the sodium Raman clock studies, the central Ramsey fringe associated with the magnetic field insensitive m = 0, δ m = 0 transition can be used as a reference for the stabilization of the microwave oscillator. The Raman clock would have an advantage over the conventional cesium clock, in that it does not require state selection magnets, nor a microwave cavity.

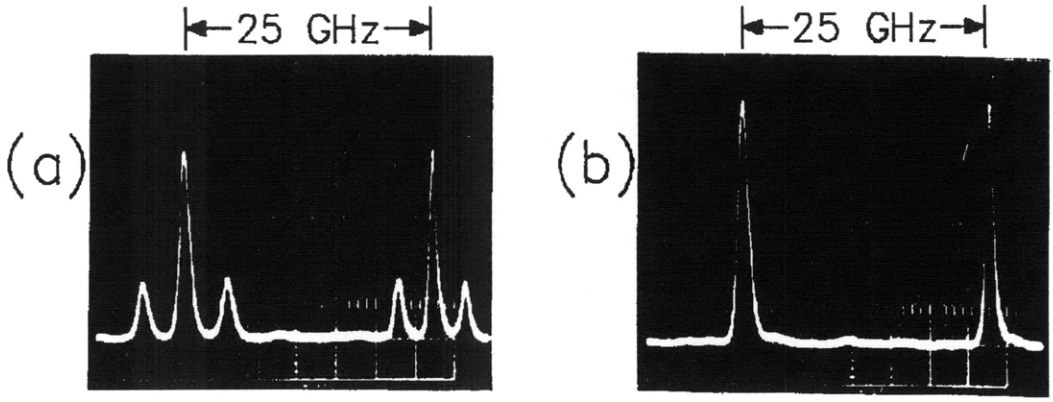

Figure 22.4 Spectrum of: (a) Modulated laser at 4.6 GHz (b) Unmodulated laser.

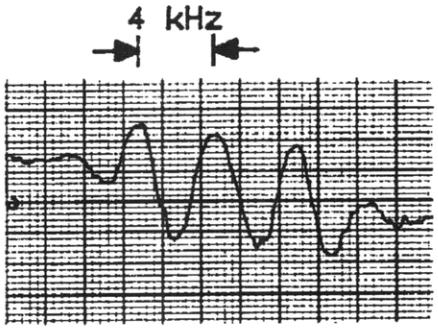

Figure 22.5 Ramsey fringes for a 7.5 cm zone separation.

Although optical pumping has recently been considered as a replacement for the state selection magnets in the conventional cesium clock, the microwave cavity, however, is still needed.

Future work will be focused on the study of error sources in semiconductor excited cesium Raman clocks. In addition, several improvements to our present setup are being considered. For example, we propose to use a laser with a spectral width equal to or less than the cesium natural width of 5 MHz instead of the present 45 MHz. Also, we wish to consider simple methods of laser cooling the cesium beam, to increase the transit time for a given zone separation and oven temperature.

Since semiconductor lasers are also available at 780 nm near the resonance excitation of rubidium, it would be worthwhile to consider a rubidium Raman clock in addition to cesium. Finally, the possibility of a millimeter wave Raman clock is also being explored.

Publication

Hemmer, P.R., H. Lamela-Rivera, S.P. Smith, B.E. Bernacki, and S. Ezekiel, "Observation of Ultra-Narrow Ramsey Raman Fringes in a Cesium Atomic Beam Using a Semiconductor Laser," submitted to *Optics Lett.*

22.3 Coupled Pendulum Model of the Stimulated Resonance Raman Effect

The stimulated resonance Raman effect has found numerous potential applications in such diverse areas as spectroscopy, collisional studies and Raman lasers. In addition, we are exploring the possibility of using the stimulated resonance Raman interaction for portable clock development (see section 22.2 above). To date, there has not been a simple physical model to describe this interaction. Theoretical treatments using either perturbation theory or dressed states have been devised. The dressed state approach has been more successful because it describes the existence of a "trapped state" which is transparent to resonant excitation fields. This accounts for the non-absorption resonances which have been observed experimentally by a number of researchers. However, these models do not offer a simple physical explanation of either the formation of the trapped state or the influence of experimental conditions on observables.

In our research we have shown that the analogy between the stimulated resonance Raman interaction and the well-known system of three classical coupled pendulums can provide considerable physical insight. A set of three classical coupled pendulums is used to model the stimulated resonance Raman interaction. This model provides a simple, intuitive, physical description of the resonance Raman process and can also be used to interpret experimental observations, including the dynamics of Raman induced transparency, the physical nature of Ramsey fringes in separated field excitation, and the effects of off-resonant laser excitation. The model has also been extended to suggest what might be observed for very strong laser fields.

Publication

Hemmer, P.R., and M.G. Prentiss, "Coupled Pendulum Model of the Stimulated Resonance Raman Effect," submitted to *J. Opt. Soc. Am. B.*

22.4 Laser Raman Clock Using Sodium

We have continued our precision studies of dye laser induced stimulated resonance Raman interactions in a sodium atomic beam with emphasis on Ramsey's method of separated oscillatory fields. We observed Raman-Ramsey fringes for a field separation of up to 30 cm, and the data were consistent with theoretical predictions. We have also been investigating the performance of a clock based on this interaction in a sodium atomic beam to determine the feasibility of such a scheme and to demonstrate any possible advantages over conventional microwave excited clocks. Recent performance of our sodium Raman clock showed a stability of 1×10^{-11} for a 5000 second averaging time. This compares favorably with commercial cesium clocks when difference in atom transit time and transition frequency are taken into consideration.

Currently we are studying potential sources of long term frequency error in a Raman clock. Some of the error sources are similar to those in microwave clocks, such as the effects of path length shift, external magnetic fields, background slope, atomic beam misalignment and second order Doppler. The other error sources are unique to the Raman clock and include laser frequency detuning, laser intensity changes, laser beam misalignment, optical atomic recoil, the presence of nearby hyperfine levels, and other small effects.

Recently we have performed theoretical and experimental studies of an important error source related to Ramsey fringe phaseshift as a function of laser detuning in a two zone Raman excitation scheme. In our set up, laser detuning arises from many reasons such as laser drift away from the optical resonance (see section 22.2 above), misalignment of beams, and so on. Experimentally, we found that the Ramsey fringe phase shift depends strongly on initial state preparation, as well as, laser intensity in the interaction regions. We have used the Bloch vector approach to model the Raman interaction in the separated field excitation and have found that the observed phase shift is simply the phase of the 1-3 off-diagonal density matrix element at the end of the first interaction zone. This phase shift is therefore of fundamental interest and, in fact, is directly related to the phase difference between the atom-field dressed states.

The model we developed renders the Raman system almost as simple as the two level microwave system, and yet is complete enough to predict experimental observables with quantitative accuracy. Figures 22.6 (a) and 22.6 (b) show experimentally observed shift in the clock frequency as a function of laser detuning under two different sets of conditions. Figure 22.6 (c) and 22.6 (d) show theoretical predictions, according to our model, of the frequency shift we should expect corresponding to the same conditions. As can be seen, the results agree quite well both qualitatively and quantitatively. Moreover, we have verified this agreement over a wide range of parameters.

Specifically, we have investigated the effects of varying, independently, the initial population difference between levels 1 and 3 and the laser intensity in the interaction zones. Figures 22.6 (b) and 22.6 (d) correspond to a large initial population difference and low intensity. As can be seen, the clock frequency is extremely sensitive to laser detuning under this condition. Theory predicts, as shown in figure 22.6 (c), that this sensitivity becomes very small for small detuning if we use high intensity along with a small difference in population. Figure 22.6 (a) confirms this experimentally.

In summary, we are now able to choose operating conditions under which the clock is least sensitive to laser detuning. Theory also shows that under such conditions, the clock is also least sensitive to changes in laser intensity and population difference.

Our current atomic beam design is such that we were not able to run the clock under such an optimal condition. We recently finished construction of a new beam that will run under the desired conditions. Moreover, the new beam is designed to have increased signal-to-noise ratio, be more stable, and be less sensitive to external magnetic fields.

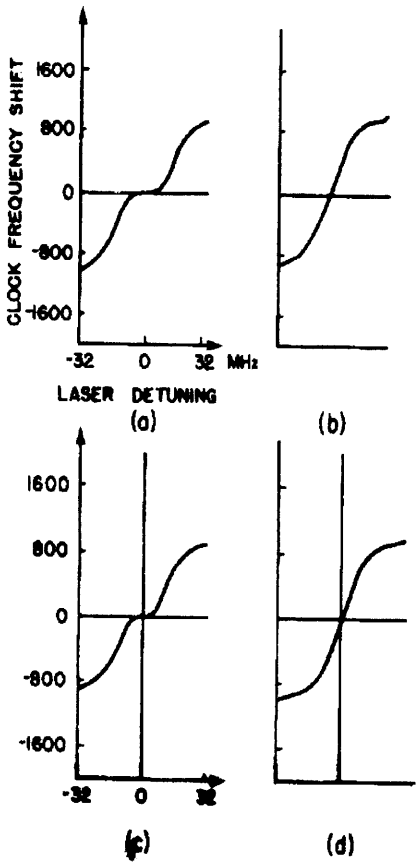

Figure 22.6 Comparison of experimental results with theoretical predictions of Raman clock frequency shift as a function of laser detuning.

22.5 Alignment Insensitive Technique for Wideband and Tuning of an Unmodified Semiconductor Laser

Many applications such as laser spectroscopy, optical pumping and isotope separation require a tunable narrow-linewidth source in the near infrared. Semiconductor lasers are an attractive alternative for these applications due to their relatively low cost, small size, and simplicity of operation. However, to date, semiconductor lasers have found limited spectroscopic applications because of their inability to be tuned to arbitrary frequencies of interest within the laser gain curve. To alleviate this problem, optical feedback schemes have been devised using diffraction gratings or etalons to provide frequency selective feedback. However, all these techniques require the use of antireflection-coated lasers and, in addition, are very sensitive to alignment of the external optics. These factors detract from the simplicity and low cost aspects inherent in semiconductor lasers.

We have developed a simple optical feedback technique that permits an ordinary semiconductor diode laser with no antireflection-coated facets to be tuned to arbitrary frequencies within the laser gain curve. In addition, this method is not highly sensitive to optical misalignments. Briefly, a one piece cat's eye retro-reflector serves as the

feedback mirror and a tilted intra-cavity solid etalon provides frequency selectivity. The use of a one piece retro-reflector contributes greatly to the simplicity of the technique because it eliminates the need for angular adjustment of the feedback mirror. The etalon, having approximately one-fifth the optical thickness of the semiconductor laser, forces the laser to lase in the longitudinal mode of interest.

Using our set up we were able to excite the D_2 line in atomic Cesium very repeatably using a nominally 852 nm laser. If the laser were used without feedback, it would not have been possible to excite the cesium transition reliably using either injection current or temperature tuning.

Publication

Bernacki, B.E., P.R. Hemmer, S.P. Smith and S. Ezekiel, "Alignment Insensitive Technique for Wideband Tuning of an Unmodified Semiconductor Laser," submitted to *Optics Lett.*

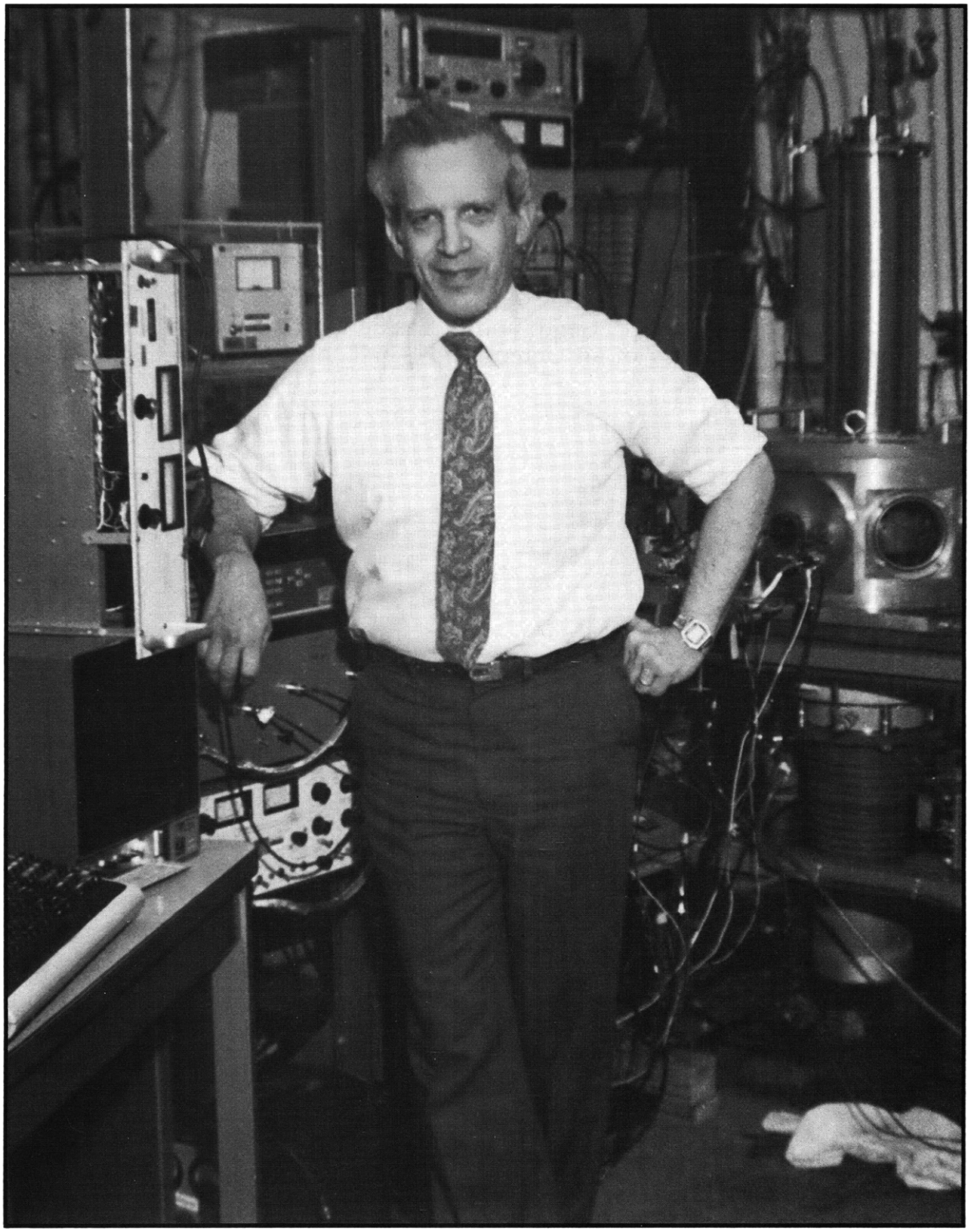

Professor Daniel Kleppner